



Microstructural evolution and sintering kinetics during spark plasma sintering of Fe and Al blended powder

Rui-di LI¹, Tie-chui YUAN¹, Xiao-jun LIU¹, Ji-wei WANG², Hong WU¹, Fan-hao ZENG¹, Xiang ZHOU¹

1. State Key Laboratory of Powder Metallurgy, Central South University, Changsha 410083, China;

2. Shenzhen Institute of Information Technology, Shenzhen 518172, China

Received 7 March 2016; accepted 23 February 2017

Abstract: The reaction diffusion between Fe and Al during spark plasma sintering (SPS) was studied. Microstructural evolution was investigated by X-ray diffraction (XRD) and scanning electron microscopy (SEM) and the sintering kinetics was disclosed. The main interphase of the SPS sample was Fe_2Al_5 at 773–873 K. Ball-milling enabled a large number of lattice defects and grain boundaries thus the reaction kinetics was accelerated, although the direct current can also promote those defects. After milling, the phase transformation kinetics was improved from 0.207 before mill to 4.56×10^{-3} . Besides, this work provided more details for the generation of Joule heating. The resistance offered to the electric path was considered to be the source of Joule heating, and particularly the resistance offered by the different contact interfaces of die, punch, graphite foil and the sample played a leading role for the generation of Joule heating during spark plasma sintering.

Key words: Fe–Al blended powder; spark plasma sintering; sintering kinetics; diffusion; reaction; Joule heating

1 Introduction

Recently, spark plasma sintering (SPS), as a newly developed sintering process, has been widely applied for the synthesis and consolidation of various materials such as metals and alloys, intermetallic, ceramics, metal–ceramic and ceramic–ceramic composites [1–4]. Compared with other conventional sintering process including pressureless sintering, hot-pressing and others, the SPS process presented significant advantages: high heating rate, lower sintering temperature, shorter holding time and marked comparative improvement in properties of materials [5]. Therefore, SPS process is thought to be an advanced rapid sintering technique and used to prepare all kinds of materials. MIRAZIMI et al [3] reported that SPS can not only enable fully densification but also retain ultrafine grains of dense nanostructured Fe–Al alloy. BERNARD et al [6] reported the acquirement of dense nanostructured intermetallic. Although plentiful works have been made to study the

relationships between SPS parameters, microstructures and properties of various materials [7–10], the knowledge available for the sintering mechanism is insufficient. Owing to the simultaneous existence of pressing, thermal, electromagnetic fields and their complicated coupling effects in SPS process [11–14], the interaction mechanisms between particles are debatable, therefore the sintering mechanism cannot be well understood [5,15–17].

Actually, interface reaction is the minimal scaled dynamics behavior in sintering process, by which the discrete particles evolve into dense metallic part. Moreover, the rapid densification and outstanding performances of various materials during SPS process may correlate with atomic diffusion under the complex conditions of press, temperature, pulsed DC current and possible electromagnetic field. Previous work studied the atomic diffusion behavior of Fe–Al diffusion couples in the presence of pulse current [18]. BONIFACIO et al [15] revealed the dielectric breakdown of surface oxides during the SPS diffusion. KONDO et al [19] studied the

Foundation item: Projects (51474245, 51571214) supported by the National Natural Science Foundation of China; Projects (2015GK3004, 2015JC3006) supported by the Science and Technology Project of Hunan Province, China; Project (2016YFB1100101) supported by the National Key Research and Development Program, China; Project (K1502003-11) supported by the Changsha Municipal Major Science and Technology Program, China; Project (CSUZC2015030) supported by the Open-End Fund for the Valuable and Precision Instruments of CSU, China; Projects (2015CX004, 2016CX003) supported by the Project of Innovation-driven Plan in CSU, China

Corresponding author: Tie-chui YUAN; Tel/Fax: +86-731-88830142; E-mail: tiechuiyuan@csu.edu.cn

DOI: 10.1016/S1003-6326(17)60181-X

effect of DC current on atomic diffusion. However, in consideration of the difference between the diffusion couples and powder sintering, it is necessary to investigate the reaction diffusion behavior between powder particles in SPS process.

In this experiment, Fe and Al powder mixtures were used to investigate the microstructural evolution and sintering kinetics in SPS process. The selection of the Fe and Al powder mixtures was due to the lower cost and its good prospect [4,20]. The aim of this work is to study the microstructure evolution and atomic diffusion of Fe–Al blend powder in SPS process. The effects of sintering conditions on the interface reaction of Fe–Al powder mixture was studied. Meanwhile, the resistance role of the graphite die, sample, and the mutual interfaces for producing Joule heating was also investigated.

2 Experimental

2.1 Preparation of mixed powders

The commercial-purity Fe (99.5% purity) powders with an average particle size of 70 μm and Al (25 μm , 99.9% purity) were used as raw materials of this study to be sintered by the SPS apparatus (FCT D25/3, Germany). All the elemental powders below were prepared with the composition of 60% Fe and 40% Al (mole fraction). In order to study the effect of microstructure on reactive diffusion, two types of mixed powder were prepared before the sintering process. The first type of mixed powder was prepared from the as-received powders according to the proportion above (referred to as-received mixed powders below). As to the second type of mixed powders, the as-received Fe powders were milled inside a planetary stainless steel ball mill at 200 r/min for 20 h. The ball-to-powder mass ratio was about 5:1. In order to minimize oxygen contamination, the ethanol was used as the milling medium. Then blending the Fe powders after ball-milling and Al powders obtained the second type of mixed powders (referred to as-milled mixed powders below).

2.2 SPS process

The pre-mixed powders was consolidated using the SPS apparatus (FCT D25/3, Germany) under a vacuum condition (~ 5 Pa) by following procedure. First, approximately 8 g of powder was loaded into a high-density graphite die with a 20 mm internal diameter. Thin graphite foils were placed between powders and graphite die surfaces to prevent welding and obtain a more uniform current flow. Second, the powders were prepressed in the graphite die under a loading about 40 MPa to obtain a compact form before SPS processing. Third, a sintering pressure of 40 MPa was applied before heating and held until the end of sintering program.

During the sintering, the temperature was measured by two different means serviced for the program: thermocouple temperature below 673 K and infrared thermometer above 673 K.

This study is to investigate the behavior of reaction diffusion between Fe and Al via a solid-state reaction, so the sintering temperature should be limited below the melting point of aluminum. Accordingly, the samples were heated at different temperatures (773, 798, 823, 873 K) at a rate of 100 K/min and held for 10 to 120 min. After completion of the sintering step, the samples were cooled down to ambient temperature.

2.3 Characterization

The sintered samples of two types of mixed powders by spark plasma sintering were characterized using scanning electron microscopy (SEM), X-ray diffraction (XRD). X-ray diffraction was used to analyze the type of phases formed during the sintering. Back-scattering images in scanning electron microscopy were used to analyze the process of phased formed. The volume fraction of the reaction layers formed was evaluated from SEM images by means of image analysis software (Image Pro Plus).

3 Results and discussion

3.1 Growth behavior of intermetallic compound during SPS

The evolution of Fe–Al intermetallic was observed by SEM in the back scattered electron (BSE) imaging mode. Figure 1(a) shows the microstructure sintered at 773 K for 90 min. The bright and dark areas refer to Fe and Al, respectively. Figures 1(b) and (c) show the microstructures sintered at 798 K and 823 K for 30 min. It is obvious that the consumption of aluminum during the reaction process in the sample sintered at 823 K is more rapid than that at 798 K. Moreover, the thickness of grey layer increased markedly when temperature rose from 798 K (thickness about 10 μm) to 823 K (thickness about 16 μm). Figure 1(d) shows the microstructure of specimen sintered at 873 K for 5 min. Noted that at this temperature, aluminum was consumed very fast. Extending the heat preservation time to 30 min, the XRD confirmed that aluminum existed in the sample, as shown in Fig. 2.

It can be found that in Fig. 1(d), a large number of pores exist along phase boundaries. There are almost no obvious pores in the samples at low temperature of 773 K while the pores formed at a high temperature of 873 K. In view of the difference in diffusion coefficient of Fe and Al, it can be concluded that the formation of pores is attributed to the Kirkendall effect and the changes in volumes during reaction [1,21,22].

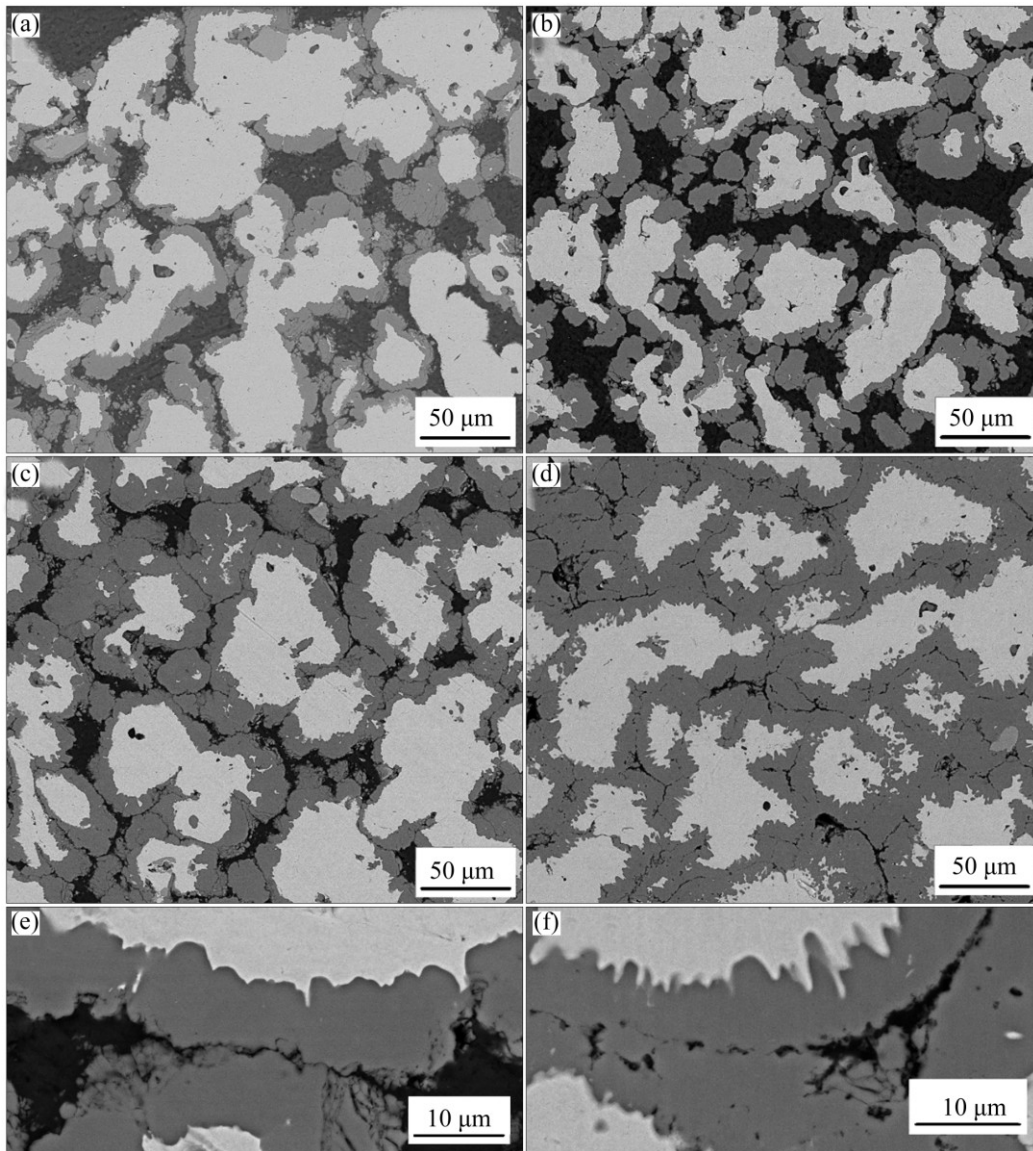


Fig. 1 Backscattered electron images of consolidated samples (as-received) sintered at different temperatures: (a) 773 K for 90 min; (b) 798 K for 30 min; (c) 823 K for 30 min; (d) 873 K for 5 min; (e) High magnification of (c); (f) High magnification of (d)

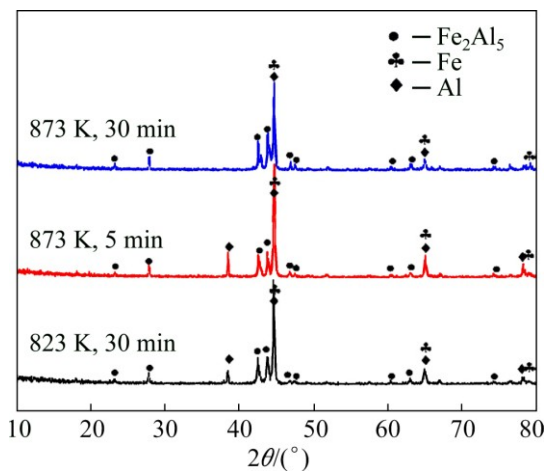


Fig. 2 X-ray diffraction patterns of samples sintered at 823 K for 30 min, 873 K for 5 and 30 min by SPS

Figures 1(e) and (f) are high magnification images of Figs. 1(c) and (d), respectively. Figures 1(e) and (f) both clearly show that the reaction layers are continuous but their thicknesses vary along the baseline. At the interface between reaction layer and Fe, a well-known large-scale wavy features are clearly visible [23–25]. Compared with the relative smoothness interface of Fig. 1(e), the interface between the reaction layer and Fe in Fig. 1(f) displayed more irregular.

In this experiment, the interface reaction between Fe and Al particle starts with the formation of intermetallic (the grey layer). According to the EDS analysis together with the X-ray diffraction results (Fig. 2), it can be concluded that these grey layers are the Fe_2Al_5 phase.

According to Fe–Al phase diagram [26], FeAl_3 ,

FeAl₂ and FeAl as well as Fe₂Al₅ appear as stable intermetallic compounds at temperature ranging from 823 to 913 K. JÓZWIAK et al [27] found that a heating rate lower than 2.5 K/min yields the phase transformation sequences as Fe+Al→FeAl₃→Fe₂Al₅→FeAl₂→FeAl, consistent with the binary phase diagram of Fe–Al. However, FeAl₃, FeAl₂ and FeAl phases were not observed in any sintering samples in present study. It may be attributed to the high heating rate (100 K/min in present study) of SPS and the slower nucleation and growth rate of FeAl₃, FeAl₂ and FeAl compared with Fe₂Al₅. Consequently, FeAl₃, FeAl₂ and FeAl cannot grow to visible thicknesses within the experimental conditions.

Figure 3 shows that the volume fractions of reaction layer (Fe₂Al₅) vary with holding time under different sintering temperatures. X_T refers to the volume fractions of Fe₂Al₅ layer measured by SEM image analysis, which can represent the reaction extent between the Fe and Al powder particles. The theoretical volume fraction of the Fe₂Al₅ phase is expected to be 62.18%. But in consideration of the loss by ball-milling, the final volume fraction is smaller than the theoretical one. When the SPS was performed at 773 K, the reaction diffusion is very slow and elevating temperature makes the reaction more rapidly. It can be explained by the Arrhenius equation [20,26].

$$D=D_0 \exp[-Q/(RT)] \quad (1)$$

where D_0 and R are the diffusion constant and gas constant, respectively. And Q is the activation energy.

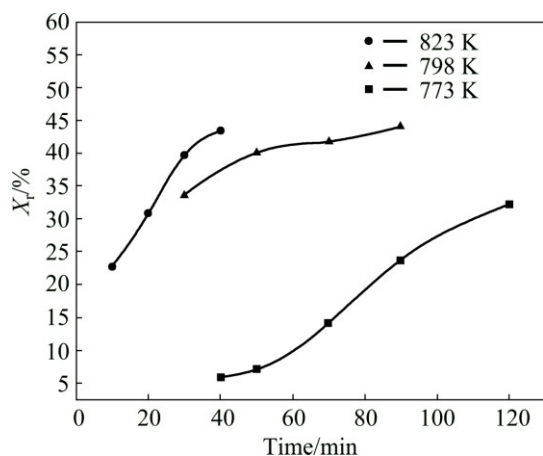


Fig. 3 Volume fractions (X_T) of reaction layer (Fe₂Al₅) measured versus time at 773 K, 798 K and 823 K

The temperature is the main factor influencing the diffusion rate. When raising the reaction temperature, atom migration becomes easier due to the increase of the vibrational frequency. In this work, the influence of electric field on the diffusion coefficient should be considered. Previous literatures pointed out that the

existence of electric field may reduce the activation energy required for atom migration [5,11,13,17]. It is not possible from current study to comment on the atomistic mechanisms responsible for reduction of the activation energy for diffusion in the presence of electric field.

3.2 Effect of ball-milling on growth behavior of intermetallic compound

Figure 4(a) shows the SEM image of sample (as-milled) sintered at 823 K. The EDS Fig. 4(b) shows that the molar ratio of reaction layers conforms to Fe₂Al₅ phase. Ball-milling enables more rapid reaction than mixed powders (Fig. 5(a)). This is because that there exist a large number of crystal defects such as high dislocation or vacancy density after balling mill.

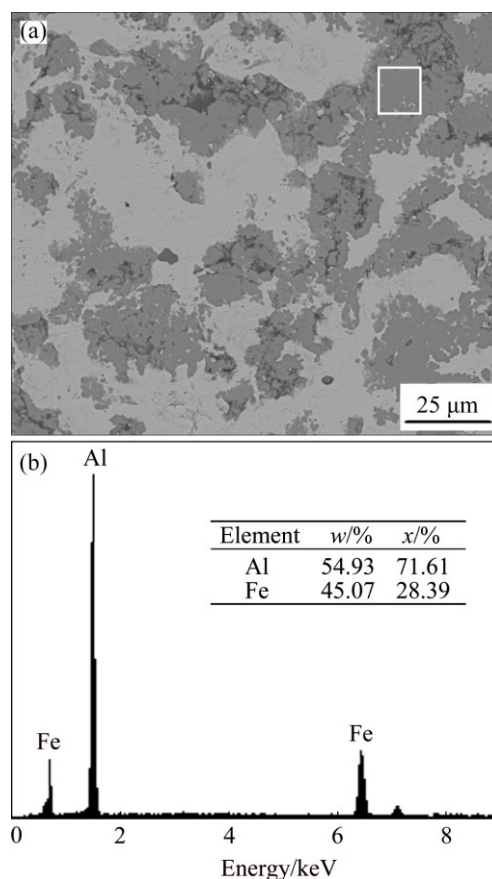


Fig. 4 Backscattered electron image (a) and corresponding EDS results (b) of consolidated samples (as-milled) sintered at 823 K for 30 min

According to the Johnson–Mehl–Avrami (JMA) kinetics [20], the equation can be expressed as follows:

$$\zeta=1-\exp(-kt^n) \quad (2)$$

where k and n are constants with respect to time, t . ζ refers to the fractional extent of crystallization dependent of time. Equation (2) can also be written in following form:

$$\ln[\ln(1/(1-\zeta))]=\ln k+n \ln t \quad (3)$$

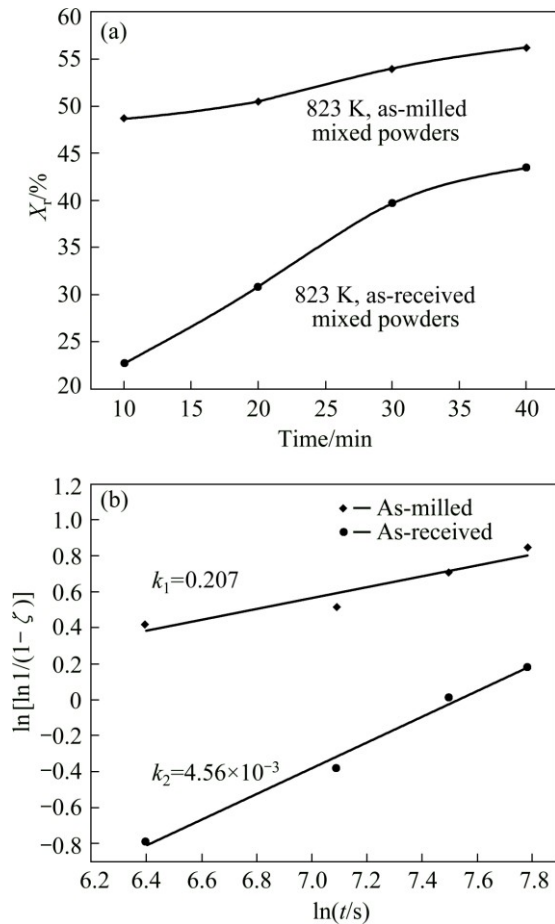


Fig. 5 Volume fractions (X_T) of reaction layer (Fe_2Al_5) measured versus time by sintering as-received and as-milled powders at 823 K (a), and plot of $\ln[\ln 1/(1-\zeta)]$ vs $\ln t$ at 823 K for as-received and as-milled powders (b)

Previous studies reported that Eq. (2) or (3) can be used to describe the transformation kinetics of many solid state processes under isothermal conditions. Thus, the value of k can be obtained according to Eq. (3), as shown in Fig. 5(b).

In Fig. 5(b), k_1 refers to the reaction rate of the as-milled mixed powders at 823 K, and k_2 refers to the reaction rate of as-received SPS blend powder. As shown in Fig. 5(b), the values of k_1 and k_2 are 0.207 and 4.56×10^{-3} , respectively. It can be seen that k_2 is almost two orders of magnitude lower than k_1 . Two factors contribute the faster diffusion of “as-milled” samples than “as-received” samples. First, during ball milling process, a large number of lattice defects generate owing to severe deformation, which provides more diffusion paths. Second, current supplied for Joule heating passes through the graphite and sample. The current enhances the atom mobility.

3.3 Analysis of current during reaction diffusion of SPS

Figures 6(a) and (b) present the BSE images of

compact discs (as-received and as-milled, respectively) sintered at 773 K for 70 min. It is clear that the Fe_2Al_5 phase only appeared on partial iron particles, but not appeared on every iron particles. Moreover, with the increase of holding time to 50, 70, 90, 120 min, those iron particles without Fe_2Al_5 phase covered on the surface become less and less until disappear when reaching up to 120 min. This phenomenon can be attributed to the specialization of SPS: heating method.

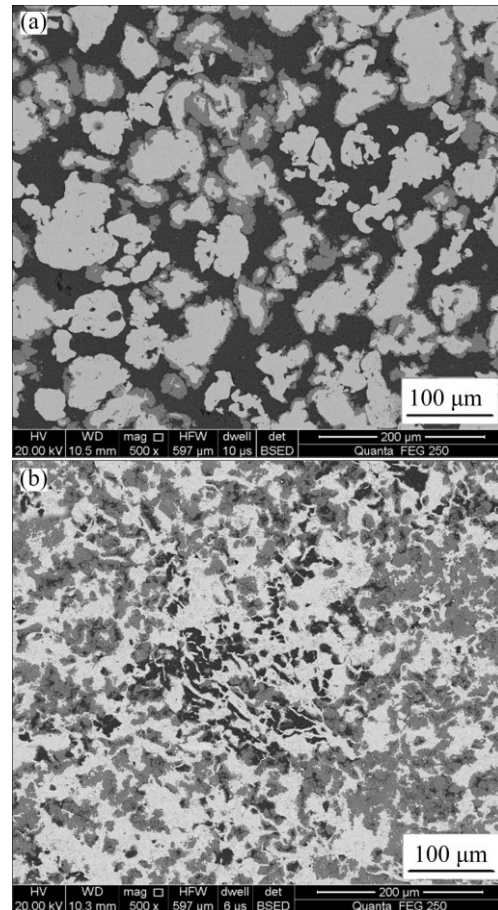


Fig. 6 Backscattered electron images of consolidated samples sintered at 773 K for 70 min: (a) As-received; (b) As-milled

As it is widely known, differing from conventional heating by thermal radiation, the target temperature in SPS depends on the Joule heating generated in the die (typical graphite) and the samples because of the current density offered to the electric path. It is sure that the compact disc of blended powder of iron and aluminum can be a good conductor but not an idealized conductor due to many factors, such as inconformity of powder particles size, shape and difference of contact resistance caused by the inconformity. Those factors lead to inhomogeneous distribution of current density, which further cause the above phenomenon. When increasing the temperature to 798 K or even higher, the phenomenon does not appear. This is because that increasing temperature requires greater applying current,

which leads to the entire increase in current density even though inhomogeneous distribution of current density. Figure 7 presents the current changes during SPS process at different temperatures. In the holding stage (*C* section in Fig. 7), the current basically keeps steady. As to the two points (*A* and *B* in Fig. 7), it is because of the switch of temperature measure method from thermocouple to infrared thermometry which depends on the sintering unit. Since the switch occurs at temperature below 673 K (the lowest temperature of the infrared temperature measurement), its influence can be ignored. It is clear that the applying current at higher temperature is greater than that at lower temperature. It can be concluded that the current flowing through the electrical path is not only inhomogeneous distribution between the graphite die and the sample, which was reported in a previous literature [11], but also inhomogeneous distribution between the particles inside the sample.

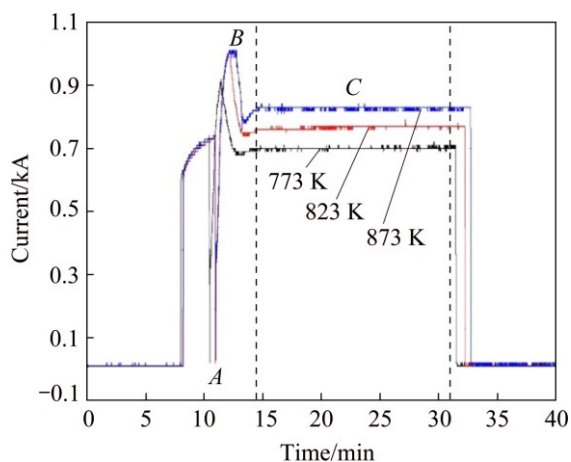


Fig. 7 Variation of current versus time during SPS

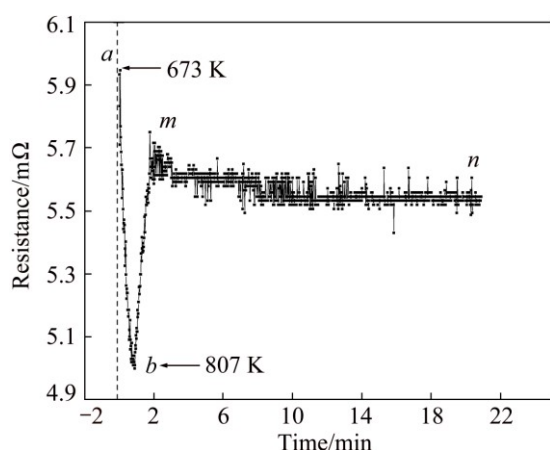


Fig. 8 Variation of resistance offered to electric path versus time at 823 K

During SPS, the existence of plasma still remains doubtful, and on the other hand, the Joule heating is thought to be a promising heat generation mechanism in the case of metal which occurs due to resistance offered

to the electric path. As discussed above, the distribution of current is inhomogeneous on the macro or micro scale. Thus, further understanding of the generation of Joule heating will be of great significance. During heating, the current supplied is not a constant but changes within a certain small range. This is because the resistance offered to electric path keeps continuously changing over time. CHAWAKE et al [16] pointed out that the Joule heating occurring at particle–particle contacts plays a significant role in the sintering of metal powders, whose analysis can be summarized into two aspects: firstly, in the initial stages of sintering, the resistance is higher which may be due to the contribution of large number of particle–particle contacts (pure metal powders) in addition to other contacts (graphite die-foil, punch-graphite foil and graphite foil-powder). Then, after the sample achieves a critical relative density, the resistance offered to the electric path by particle–particle contacts decreases and meanwhile the resistance by graphite foil, graphite die, and the punch is dominant and keeping basically stable.

In agreement with previous study, analogous results can be seen in Fig. 8. It showed the variation of total resistance offered to electric path over time. In consideration of the limitation by the infrared temperature measurement, the related data in the sintering stage after the temperature reaching 673 K was collected and analyzed. As shown in Fig. 8, the resistance in the stage (*ab*) sharply decreased to $\sim 5.01 \times 10^{-3} \Omega$ ($R_1 = R_{\text{punch}} + R_{\text{punch-foil}} + R_{\text{foil-sample}} + R_{\text{particle-particle}}$) which could be due to the relative density of sample achieves the critical point under the joint influence of sintering pressure and temperature. And differing from results by CHAWAKE et al [16], the resistance after sample achieves a certain relative density does not keep steady but increases in small increments as shown in stage (*bm*). It is because the elemental powders, comparing to the pure metal powders in literature, could perform mutual diffusion reaction to form new phases at the interface of different elemental powder particles. In this experiment, Fe and Al mixed powders are used and reaction diffusion leads to the formation of new phase- Fe_2Al_5 in the stage (*bm*). Due to the formation of Fe_2Al_5 , many new interfaces are obtained between Fe_2Al_5 layers and powder particles (Fe and Al particles) where there is an abrupt change in materials and lead to increased resistance to $5.75 \times 10^{-3} \Omega$ ($R_1 + R_{\text{interphase-Fe}} + R_{\text{interphase-Al}}$). Then, in the stage (*mn*), the resistance keeps basically steady and declines slowly. This decline is due to the continuous reduction of Al- Fe_2Al_5 interfaces ($R_{\text{interphase-Al}}$) with the consumption of Al phase during the sintering.

From above analysis, it can be concluded that the generation of Joule heating could be attributed to the

impressed current flowing through resistance. The resistance ($\sim 5.01 \times 10^{-3} \Omega$) offered by the contacts of graphite die, punch, foil and sample plays a leading role, but the influence of resistance by the particle–particle contacts cannot be neglected.

4 Conclusions

1) The existence of current does not change the prior formation of Fe_2Al_5 phase which accorded with many previous studies. Meanwhile, raising temperature even in a small range could promote reaction diffusion between the Fe and Al powders.

2) By ball milling, the diffusion reaction rate became quicker because the ball-milling provided more defects. After milling, the phase transformation kinetics was improved from 0.207 without mill to 4.56×10^{-3} .

3) During SPS, the generation of Joule heating was derived from the current. The current offered to electric path is not only inhomogeneous distribution between the graphite die and the sample, but also inhomogeneous distribution between the particles inside the sample, and the resistance offered by the different interfaces due to the mutual contacts of die, graphite foil and the sample played a leading role in the generation of Joule heating.

References

- [1] SUN Y, KULKARNI K, SACHDEV A K, LAVERNIA E J. Synthesis of γ -TiAl by reactive spark plasma sintering of cryomilled Ti and Al powder blend, Part I: Influence of processing and microstructural evolution [J]. *Metallurgical and Materials Transactions A*, 2014, 45(6): 2750–2758.
- [2] SIWAK P, GARBIEC D. Microstructure and mechanical properties of WC–Co, WC–Co– Cr_3C_2 and WC–Co–TaC cermets fabricated by spark plasma sintering [J]. *Transactions of Nonferrous Metals Society of China*, 2016, 26(10): 2641–2646.
- [3] MIRAZIMI J, ABACHI P, PURAZRANG K. Microstructural characterization and dry sliding wear behavior of spark plasma sintered Cu-YSZ composites [J]. *Transactions of Nonferrous Metals Society of China*, 2016, 26(7): 1745–1754.
- [4] ORRÚ R, LICHERI R, LOCCI A M, CINCOTTI A, CAO G. Consolidation/synthesis of materials by electric current activated/assisted sintering [J]. *Materials Science and Engineering R*, 2009, 63(4–6): 127–287.
- [5] MUNIR Z A, ANSELMITAMBURINI U, OHYANAGI M. The effect of electric field and pressure on the synthesis and consolidation of materials: A review of the spark plasma sintering method [J]. *Journal of Materials Science*, 2006, 41(3): 763–777.
- [6] BERNARD F, LE GALLET S, SPINASSOU N, PARIS S, GAFFET E, WOOLMAN J N. Dense nanostructured materials obtained by spark plasma sintering and field activated pressure assisted synthesis starting from mechanically activated powder mixtures [J]. *Science of Sintering*, 2004, 36(3): 155–164.
- [7] ZHAO L D, ZHANG B P, LI J F, ZHANG H L, LIU W S. Enhanced thermoelectric and mechanical properties in textured n-type Bi_2Te_3 prepared by spark plasma sintering [J]. *Solid State Sciences*, 2008, 10(5): 651–658.
- [8] SCITI D, MONTEVERDE F, GUICCIARDI S, PEZZOTTI G, BELLOSI A. Microstructure and mechanical properties of ZrB_2 - MoSi_2 ceramic composites produced by different sintering techniques [J]. *Materials Science and Engineering A*, 2006, 434(1–2): 303–309.
- [9] CHA S I, HONG S H. Microstructures of binderless tungsten carbides sintered by spark plasma sintering process [J]. *Materials Science and Engineering A*, 2003, 356(1–2): 381–389.
- [10] ZHAN G, KUNTZ J, WAN J, GARAY J, MUKHERJEE A K. Alumina-based nanocomposites consolidated by spark plasma sintering [J]. *Scripta Materialia*, 2002, 47(11): 737–741.
- [11] ANSELMITAMBURINI U, GENNARI S, GARAY J E, MUNIR Z A. Fundamental investigations on the spark plasma sintering/synthesis process [J]. *Materials Science and Engineering A*, 2005, 394(1–2): 139–148.
- [12] CHEN W, ANSELMITAMBURINI U, GARAY J E, GROZA J R, MUNIR Z A. Fundamental investigations on the spark plasma sintering/synthesis process-I. Effect of dc pulsing on reactivity [J]. *Materials Science and Engineering A*, 2005, 394(1–2): 132–138.
- [13] ANSELMITAMBURINI U, GARAY J E, MUNIR Z A. Fundamental investigations on the spark plasma sintering/synthesis process III. Current effect on reactivity [J]. *Materials Science and Engineering A*, 2005, 407(1–2): 24–30.
- [14] ANSELMITAMBURINI U, GENNARI S, GARAY J E, MUNIR Z A. Fundamental investigations on the spark plasma sintering/synthesis process - II. Modeling of current and temperature distributions [J]. *Materials Science and Engineering: A*, 2005, 394(1–2): 139–148.
- [15] BONIFACIO C S, HOLLAND T B, van BENTHEM K. Time-dependent dielectric breakdown of surface oxides during electric-field-assisted sintering [J]. *Acta Materialia*, 2014, 63: 140–149.
- [16] CHAWAKE N, PINTO L D, SRIVASTAV A K, AKKIRAJU K, MURTY B S, KOTTADA R S. On Joule heating during spark plasma sintering of metal powders [J]. *Scripta Materialia*, 2014, 93: 52–55.
- [17] MUNIR Z A, QUACH D V, OHYANAGI M. Electric current activation of sintering: A review of the pulsed electric current sintering process [J]. *Journal of The American Ceramics Society*, 2011, 94(1): 1–19.
- [18] LI R, YUAN T, LIU X, ZHOU K. Enhanced atomic diffusion of Fe–Al diffusion couple during spark plasma sintering [J]. *Scripta Materialia*, 2016, 110: 105–108.
- [19] KONDO T, YASUHARA M, KURAMOTO T, KODERA Y, OHYANAGI M, MUNIR Z A. Effect of pulsed DC current on atomic diffusion of Nb–C diffusion couple [J]. *Journal of Materials Science*, 2008, 43(19): 6400–6405.
- [20] SUN Y, KULKARNI K, SACHDEV A K, LAVERNIA E J. Synthesis of γ -TiAl by reactive spark plasma sintering of cryomilled Ti and Al powder blend: Part II: Effects of electric field and microstructure on sintering kinetics [J]. *Metallurgical and Materials Transactions A*, 2014, 45(6): 2759–2767.
- [21] TIWARI G P, MEHROTRA R S. Kirkendall effect and mechanism of self-diffusion in B2 intermetallic compounds [J]. *Metallurgical and Materials Transactions A*, 2012, 43(10): 3654–3662.
- [22] SALAMON M, MEHRER H. Interdiffusion, Kirkendall effect, and Al self-diffusion in iron-aluminium alloys [J]. *Eitschrift Fur Metallkunde*, 2005, 96(1): 4–16.
- [23] SPRINGER H, KOSTKA A, PAYTON E J, RAABE D, KAYSSER PYZALLA A, EGGELER G. On the formation and growth of intermetallic phases during interdiffusion between low-carbon steel and aluminum alloys [J]. *Acta Materialia*, 2011, 59(4): 1586–1600.
- [24] BOUAYAD A, GEROMETTA C, BELKEBIR A, AMBARI A. Kinetic interactions between solid iron and molten aluminium [J]. *Materials Science and Engineering A*, 2003, 363(1–2): 53–61.

- [25] BOUCHE K, BARBIER F, COULET A. Intermetallic compound layer growth between solid iron and molten aluminium [J]. Materials Science and Engineering A, 1998, 249(1–2): 167–175.
- [26] NAOI D, KAJIHARA M. Growth behavior of Fe₂Al₅ during reactive diffusion between Fe and Al at solid-state temperatures [J]. Materials Science and Engineering A, 2007, 459(1–2): 375–382.
- [27] JÓZWIAK S, KARCZEWSKI K, BOJAR Z. Kinetics of reactions in FeAl synthesis studied by the DTA technique and JMA model [J]. Intermetallics, 2010, 18(7): 1332–1337.

放电等离子烧结 Fe–Al 混合粉的 显微组织演化及烧结动力学

李瑞迪¹, 袁铁锤¹, 刘晓军¹, 王基维², 吴宏¹, 曾凡浩¹, 周祥¹

1. 中南大学 粉末冶金国家重点实验室, 长沙 410083;

2. 深圳信息职业技术学院, 深圳 518172

摘要: 研究了 Fe 与 Al 混合粉在放电等离子烧结(SPS)作用下的反应扩散行为。采用 X 射线衍射及扫描电镜对显微组织演化进行了分析, 并揭示了烧结动力学行为。结果表明在 SPS 温度 773~873 K 下, Fe₂Al₅ 为反应中间相。尽管电流可以提高材料扩散速度, 球磨处理可在粉体中产生大量点阵缺陷及晶粒边界, 使反应动力学速度得到提高。球磨后, 相变动力学速度从球磨前的 4.56×10^{-3} 提高到 0.207。而且, 本研究揭示了焦耳热产生行为。作为电流通道, 阻抗是重要的焦耳热源。SPS 过程中粉末颗粒、模具、冲头、石墨纸之间界面阻抗是焦耳热产生的重要来源。

关键词: Fe–Al 混合粉; 放电等离子烧结; 烧结动力学; 扩散; 反应; 焦耳热

(Edited by Yun-bin HE)